

Phase diagram of spin-1 quantum Ising models: Applications to systems of weakly coupled classical Ising chains

Yuval Gefen

Department of Physics and Astronomy, Tel-Aviv University, Ramat Aviv, Israel

Yoseph Imry* and David Mukamel†

IBM Thomas J. Watson Research Center, Yorktown Heights, New York 10598

(Received 26 November 1980)

The global phase diagram of the $S = 1$ Ising model in a transverse field is studied using a mean-field approximation. The critical behavior has also been considered by real-space renormalization-group techniques. This model is used to analyze the phase diagram of weakly coupled ($J_{\perp}/J_{\parallel} \ll 1$) classical Blume-Emery-Griffith chains. It is found that such systems display a first-order transition only in a very limited range of their parameters.

Physical systems described by spin- S models with $S > \frac{1}{2}$ have been studied extensively in recent years.^{1,2} Examples range from magnetic systems such as CsNiCl_3 ,^{3,4} RbNiCl_3 ,⁵ TMMC [TMMC is $(\text{CD}_3)_4\text{NMnCl}_3$], and $\text{CsMnCl}_3 \cdot 2\text{H}_2\text{O}$,^{6,7} to classical fluid mixtures,⁸⁻¹³ ^3He - ^4He solutions,¹⁴⁻¹⁶ and many others.¹⁷ The phase diagrams associated with these models are rather complex, exhibiting first- and second-order transitions and a variety of multicritical points. These models have been studied using a mean-field theory,¹¹⁻¹⁵ ϵ expansion methods,¹⁸ series expansions,¹⁹ Monte Carlo techniques,²⁰ and real-space renormalization-group (RG) calculations.^{21,22} It is generally found that the predictions of the conventional mean-field theory concerning the phase diagrams and the order of the transitions are qualitatively correct for isotropic $d \geq 3$ dimensional models.

A case of particular interest is that of weakly coupled chains. Here fluctuations of the order parameter are strong and as a result the ordinary mean-field theory may fail to give a qualitatively correct phase diagram. For example, in the limit of vanishing interchain coupling the theory predicts finite transition temperatures, although the system is effectively one dimensional and it orders only at $T = 0$. In addition to the reduction of the transition temperature, the fluctuations may modify its order as well. In order to study these effects one should analyze the phase diagrams of these systems using approximations which take into account the effect of the large fluctuations. This may be done using RG techniques or high- and low-temperature series expansions. Alternatively, one may use the transfer matrix method to transform the problem into an interacting $(d-1)$ dimensional quantum-spin model.²³⁻³⁴ This model may, in turn, be solved using the mean-field approximation. This

procedure amounts to solving the single chain exactly and treating the interchain coupling in the mean-field approximation,³⁵ and is expected to yield qualitatively correct phase diagrams.

In this paper we analyze the phase diagram of a model Hamiltonian related to a d -dimensional classical system of weakly coupled chains. We first map this problem into an interacting $(d-1)$ dimensional quantum model, which we then study using mean-field methods³⁶ and approximate RG calculations.³⁶⁻³⁸ Specifically, we consider the following $S = 1$ model:

$$\mathcal{H} = -J_{\parallel} \sum_{\langle ij \rangle_{\parallel}} S_i S_j - J_{\perp} \sum_{\langle ij \rangle_{\perp}} S_i S_j + \Delta \sum_i S_i^2 - K_{\parallel} \sum_{\langle ij \rangle_{\parallel}} S_i^2 S_j^2 - K_{\perp} \sum_{\langle ij \rangle_{\perp}} S_i^2 S_j^2, \quad (1)$$

where $S_i = \pm 1, 0$, Δ is a single-site energy, J_{\parallel} and J_{\perp} are, respectively, the intrachain and interchain exchange interactions, K_{\parallel} and K_{\perp} are likewise quadrupole interactions. For simplicity, we take J_{\parallel} , J_{\perp} , K_{\parallel} , $K_{\perp} \geq 0$. The sums $\sum_{\langle ij \rangle_{\parallel}}$ and $\sum_{\langle ij \rangle_{\perp}}$ run over nearest-neighbor spins parallel and perpendicular to the chains, respectively. The Hamiltonian (1) is an anisotropic Blume-Emery-Griffiths (BEG) model.¹⁴ It has been extensively studied by mean field,¹¹⁻¹⁵ ϵ expansion,¹⁸ and real-space RG methods,^{21,22} as the simplest model whose phase diagram exhibits first-order and second-order surfaces, critical and tricritical lines, and a special Potts-type point.

The transfer matrix, M , of the model (1) along the chain direction can be written as

$$M = e^{-1/2H_{\parallel}} e^{-H_0} e^{-1/2H_{\perp}}, \quad (2a)$$

where

$$H_0 = X \sum_i S_{xi} + Z \sum_i S_{xi}^2, \quad (2b)$$

$$H_1 = Y \sum_i S_{zi}^2 - \beta J_{\perp} \sum_{\langle ij \rangle} S_{zi} S_{zj} - \beta K_{\perp} \sum_{\langle ij \rangle} S_{zi}^2 S_{zj}^2, \quad (2c)$$

and

$$S_x = \frac{1}{\sqrt{2}} \begin{pmatrix} 0 & 1 & 0 \\ 1 & 0 & 1 \\ 0 & 1 & 0 \end{pmatrix}, \quad (2d)$$

$$S_z = \begin{pmatrix} 1 & 0 & 0 \\ 0 & 0 & 0 \\ 0 & 0 & -1 \end{pmatrix}.$$

The indices i and j now run over the lattice points in the $(d-1)$ dimensional subspace. The coupling parameters are given by

$$\sinh^2 X = e^{-\beta K_{\parallel}} [\cosh(\beta J_{\parallel}) - e^{-\beta K_{\parallel}}]^{-1}, \quad (3)$$

$$e^{-2Z} = \frac{\cosh(\beta J_{\parallel})}{\sinh^2(\beta J_{\parallel})} (\cosh \beta J_{\parallel} - e^{-\beta K_{\parallel}}), \quad (4)$$

$$Y = \beta \Delta - \ln [2e^{\beta K_{\parallel}} \cosh(\beta J_{\parallel})]. \quad (5)$$

Using the Baker-Hausdorff formula,³⁹ Eq. (2) can be written as

$$M = \exp[-(H_0 + H_1) + H'] , \quad (6a)$$

where

$$H' = \frac{1}{12} [H_0, [H_0, H_1]] + \frac{1}{24} [H_1, [H_0, H_1]] + \dots \quad (6b)$$

Consider now the extremely anisotropic case $J_{\perp} \ll J_{\parallel}$. In the transition region one has $\beta J_{\parallel} \gg 1$, $\beta J_{\perp} \ll 1$. Assuming as well that $\beta K_{\perp} \ll 1$ and $\beta(\Delta - J_{\parallel} - K_{\parallel}) \ll 1$, we find that $H_0, H_1 \ll 1$. In this limit H' can be neglected, as it is of $O(H_0^3, H_1^3)$. We thus finally arrive at the following quantum model:

$$H = H_0 + H_1 = X \sum_i S_{xi} + Z \sum_i S_{xi}^2 + Y \sum_i S_{zi}^2 - \beta J_{\perp} \sum_{\langle ij \rangle} S_{zi} S_{zj} - \beta K_{\perp} \sum_{\langle ij \rangle} S_{zi}^2 S_{zj}^2. \quad (7a)$$

The ground state of Eq. (7) can be obtained using a mean-field-type approximation for the interaction terms [we emphasize that this is unrelated to the usual mean-field approximation of the classical problem (1)]. For the sake of simplicity we take $\beta K_{\perp} = 0$, and consider the Hamiltonian measured in units of βJ_{\perp} :

$$\frac{1}{\beta J_{\perp}} H = x \sum_i S_{xi} + z \sum_i S_{xi}^2 + y \sum_i S_{zi}^2 - \sum_i S_{zi} S_{zi+1}, \quad (7b)$$

where

$$x = \frac{1}{\beta J_{\perp}} X, \quad y = \frac{1}{\beta J_{\perp}} Y, \quad z = \frac{1}{\beta J_{\perp}} Z. \quad (7c)$$

In the mean-field approximation, the ground state is written as

$$\Psi_G^{\pm} = \prod_i \psi_i^{\pm}, \quad (8)$$

where ψ_i^{\pm} are spinors given by

$$\psi_i^{\pm} \equiv \begin{pmatrix} \alpha \\ \beta \\ \gamma \end{pmatrix} = \begin{pmatrix} \frac{\sqrt{q+m}}{2} \\ \sqrt{1-q} \\ \pm \frac{\sqrt{q-m}}{2} \end{pmatrix}, \quad (9a)$$

where $0 \leq m \leq q \leq 1$. The overall phase of this spinor is such that $\beta > 0$. As for the signs of α and γ , it is easy to see that the ground-state energy depends only on the relative sign of α and γ . This is due to the fact that the ground-state energy of Eq. (7) is invariant under the transformation $x \rightarrow -x$. We therefore, arbitrarily, take the $\alpha > 0$. The parameters q and m satisfy

$$q = \langle S_z^2 \rangle, \quad (9b)$$

$$m = \langle S_z \rangle, \quad (9c)$$

where $\langle \rangle$ denotes the ground-state expectation value. In the mean-field approximation one first calculates the expectation values:

$$\epsilon_{\pm}(m, q) = \frac{1}{\beta J_{\perp}} \langle \psi_{\vec{c}}^{\pm} | H | \psi_{\vec{c}}^{\pm} \rangle, \quad (10)$$

$$\epsilon_{\pm}(m, q) = z - m^2 + (y - \frac{1}{2}z)q - |x| \sqrt{1-q} (\sqrt{q+m} \pm \sqrt{q-m}) \pm \frac{1}{2}z (q^2 - m^2)^{1/2}. \quad (11)$$

Note that m and q satisfy $0 \leq m \leq q \leq 1$. In order to analyze the phase diagram associated with Eq. (11) it is instructive to first consider the plane $x=0$. In this case it is obvious that for $z < 0$ one has $\epsilon_{+}(m, q) \leq \epsilon_{-}(m, q)$ and therefore only ϵ_{+} has to be considered. Similarly, for $z > 0$ only ϵ_{-} has to be considered.

This diagram exhibits four phases: a ferromagnetic phase F in which the ground state is $\psi_i = (\alpha, 0, \gamma)$, and three paramagnetic phases $P1$, $P2$, and $P3$. The ferromagnetic phase is separated from the paramagnetic phases $P1$ and $P3$ by two critical lines

$$z = \pm 4. \quad (12)$$

As these lines are approached the parameters α and γ vary continuously satisfying $\alpha \rightarrow 1$, $\gamma \rightarrow \pm 1$, respec-

tively. The F - $P2$ transition line is first order, and is given by

$$y = \frac{1}{16}z^2 + \frac{1}{2}z + 1, \quad -4 \leq z \leq 4. \quad (13)$$

The transition between the $P1$ and $P2$ phases is first order and it occurs at

$$y = z, \quad z \geq 4. \quad (14)$$

The $P2$ - $P3$ transition,

$$y = 0, \quad z \leq -4 \quad (15)$$

is rather special. In order to analyze this transition we consider the energy

$$\epsilon_+(q, m=0) = z + qy. \quad (16)$$

It is clear that for $y > 0$ the energy is minimized by $q=0$, while for $y < 0$ the minimum occurs at $q=1$, as seen in Fig. 1. However, along the transition line, $y=0$, the energy is independent of q , and all states $(\sqrt{q}/2, \sqrt{1-q}, \sqrt{q}/2)$ are degenerate. Therefore although the ground states associated with the phases $P2$ and $P3$ are distinct, the two phases are not separated by a first-order transition. This is due to the fact that the Landau energy at the transition does not exhibit a two-well shape, as it does for ordinary first-order transitions, but is flat. For nonzero x , this degeneracy is removed in a way which eliminates the $P2$ - $P3$ transition, and the two phases constitute a single paramagnetic phase. We now analyze the

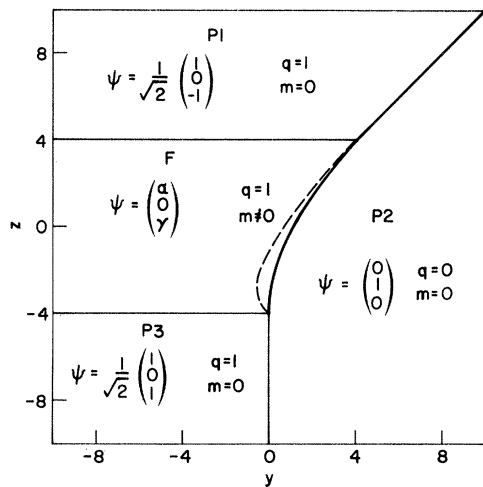


FIG. 1. Phase diagram in the $x=0$ plane, showing the ferromagnetic phase F and the three paramagnetic phases $P1$, $P2$, and $P3$. F is separated from $P1$ and $P3$ by second-order lines (thin) and from $P2$ by a first-order line (thick). $P1$ and $P2$ are separated by a first-order line. The phases $P2$ and $P3$ are distinct *only* at $x=0$. The broken line in the F phase is the projection of the tricritical line t onto the $x=0$ plane. Note that the parameters x, y, z of Eq. (7c) are used throughout the figures.

phase diagram in the three dimensional parameter space xyz . The phase diagram is given schematically in Fig. 2. It consists of three phases: a ferromagnetic phase F and two paramagnetic phases $P1$ and $P2$ ($=P3$). These phases are separated by two surfaces σ_1 and σ_2 . The σ_2 surface has a small first-order portion (the shaded area in Fig. 2) separated from the second-order part by a tricritical line t . The σ_1 surface, associated with the F - $P1$ transition, is entirely second order. We find that in the $P2$ phase the ground state is ψ_G^+ while in the $P1$ phase it is ψ_G^- . As a consequence, the σ_1 and σ_2 surfaces are associated with phase transitions in the states ψ_G^- and ψ_G^+ , respectively. An interesting property of the $P1$ phase is that the quadrupole moment attains its full value, $q=1$, throughout this phase. This is rather surprising since the operator S_x introduces a coupling between the $S_z = \pm 1$ states and the state with $S_z = 0$. However, it turns out that this coupling vanishes for the mean-field ground state of the $P1$ phase, $\psi_G^- = (1/\sqrt{2})(1, 0, -1)$. This property of the ground state is thus due to a quantum-mechanical cancellation effect.

In order to locate the two critical surfaces σ_1 and σ_2 one should first minimize $\epsilon_{\pm}(q, m)$ with respect to q . Solving the equations

$$\frac{\partial \epsilon_{\pm}(q, m)}{\partial q} = 0 \quad (17)$$

one obtains a function $q = q(m)$, which minimizes ϵ_{\pm} for a given m . Inserting $q(m)$ into $\epsilon_{\pm}(q, m)$ one obtains an expression for the energy $\epsilon_{\pm}(m)$ which

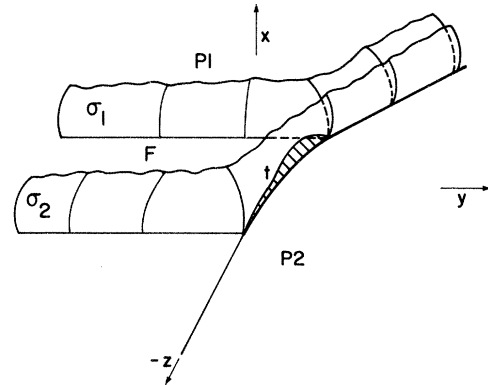


FIG. 2. Schematic phase diagram in the xyz parameter space. The phase diagram is symmetric under the transformation $x \rightarrow -x$. Only the $x > 0$ part is shown. The ferromagnetic phase F is separated from the paramagnetic phase $P1$ by a second-order surface σ_1 and from the paramagnetic phase $P2$ by a surface σ_2 . σ_2 is mostly second order but has a small first-order portion (shaded) bounded by the tricritical line t . σ_1 and σ_2 meet at the first-order line separating the phases $P1$ and $P2$ in the $x=0$ plane. For details of the σ_1 and σ_2 surfaces see Fig. 3.

depends only on m . Expanding now $\epsilon_{\pm}(m)$ in powers of m , the usual Landau expansion of the energy in the vicinity of the critical surface is obtained. In fact, due to the symmetry of the Hamiltonian (7) only terms even in m appear in this expansion.

It turns out, however that Eq. (17) is rather complicated for nonvanishing m . We therefore solve it by expanding $q(m)$ in powers of m^2 , and solving for the first few terms in the expansion. Consider first the σ_2 surface, associated with ϵ_+ . For $m=0$ we find, $q=q_0$, where q_0 satisfies the equation:

$$y + |x| \frac{2q_0 - 1}{\sqrt{q_0(1-q_0)}} = 0 . \quad (18)$$

Expanding ϵ_+ in powers of m^2 we find

$$\epsilon_+ = \sum_{k=0}^{\infty} a_{2k}^+ m^{2k} , \quad (19a)$$

where

$$a_0^+ = z + yq_0 - 2|x|\sqrt{q_0(1-q_0)} , \quad (19b)$$

$$a_2^+ = -1 + \frac{1}{4q_0^2} |x|\sqrt{q_0(1-q_0)} - \frac{1}{4q_0} z , \quad (19c)$$

$$a_4^+ = \frac{5}{64q_0^4} |x|\sqrt{q_0(1-q_0)} - \frac{1}{16q_0^3} z , \quad (19d)$$

$$a_6^+ = \frac{21}{512q_0^6} |x|\sqrt{q_0(1-q_0)} - \frac{1}{36q_0^5} z , \quad (19e)$$

and q_0 is given by Eq. (18). Using this expansion we locate the critical surface σ_2 by setting

$$a_2^+ = 0 \quad (20)$$

with

$$a_4^+ > 0 .$$

The tricritical line t is given by the equations

$$a_2^+ = a_4^+ = 0 , \quad (21)$$

with

$$a_6^+ > 0 .$$

A convenient parametric representation for the tricritical line is provided by the following equations:

$$|x| = 4(1-q_0)\sqrt{q_0(1-q_0)} , \quad (22a)$$

$$y = 4(1-q_0)(1-2q_0) , \quad (22b)$$

$$z = 4(1-3q_0+q_0^2) . \quad (22c)$$

Here q_0 is regarded as a parameter. In order to locate the critical surface σ_1 we observe that in the $P1$ phase one has $q=1$. Expanding ϵ_- in powers of m^2 we find

$$\epsilon_- = \sum_{k=0}^{\infty} a_{2k}^- m^{2k} , \quad (23a)$$

where

$$a_0^- = y , \quad (23b)$$

$$a_2^- = \frac{1}{4}z - 1 - \frac{x^2}{4(z-y)} , \quad (23c)$$

$$a_4^- = -\frac{1}{16} \frac{x^4}{(3-y)^3} + \frac{1}{16} \frac{x^2 y}{(z-y)^2} + \frac{z}{16} . \quad (23d)$$

The critical surface σ_1 is given by

$$a_2^- = 0 . \quad (24)$$

Note that throughout the surface (24) one has $a_4^- > 0$ and therefore, no tricritical line is found on this surface. Some xz sections of the phase diagram for several values of y are given in Figs. 3(a)–3(c). In these figures one finds the ferromagnetic phase F and the two paramagnetic phases $P1$ and $P2$. The intersections of the σ_1 and σ_2 surfaces with the $y = \text{const}$ planes now appear as two lines. The $P1$ - F transition is second order for all values of y . For $y < 0$ and $y > 4$ the $P2$ - F transition is also second order [see Figs. 3(a) and 3(c)]. However for $0 < y < 4$, the σ_2 surface has a small first-order portion which is connected to the second-order part by a tricritical line (t) [see Fig. 3(b)]. For large $|x|$ and z the surfaces σ_2 and σ_1 approach the planes

$$|x| = z + 2 \quad (25a)$$

and

$$|x| = z - \frac{1}{2}y - 2 , \quad (25b)$$

respectively.

We have also studied the model (7b) using the real-space quantum block spin RG method.^{29–38} In this method, the chain is divided into blocks of n spins, the intrablock Hamiltonian is diagonalized and its lowest three levels are retained, defining the new single-spin variables. New nearest-neighbor spin couplings are also generated at each step. We have performed this calculation for $d=2$ (quantum chain) and with $n=2$. The tricritical fixed point found by Hamber³⁶ and Hu³⁷ was obtained along with tricritical exponents which agree, within numerical inaccuracies, with theirs. We have also found a critical Ising-like fixed point which happens to have an exponent ν close to unity. In trying to extend these RG calculations to regions far from those fixed points we find, however, difficulties in the method. For example, working at $x=0$, one would like the RG transformation to preserve the symmetry $S_x \rightarrow -S_x$. It turns out that by retaining the three lowest levels this symmetry is broken and a nonzero value of x is generated. An ad hoc procedure to overcome this difficulty, in this special case, would be to choose states other than the three lowest ones, requiring that they have the appropriate symmetry. Furthermore, due to numerous level crossings in the full parameter space,

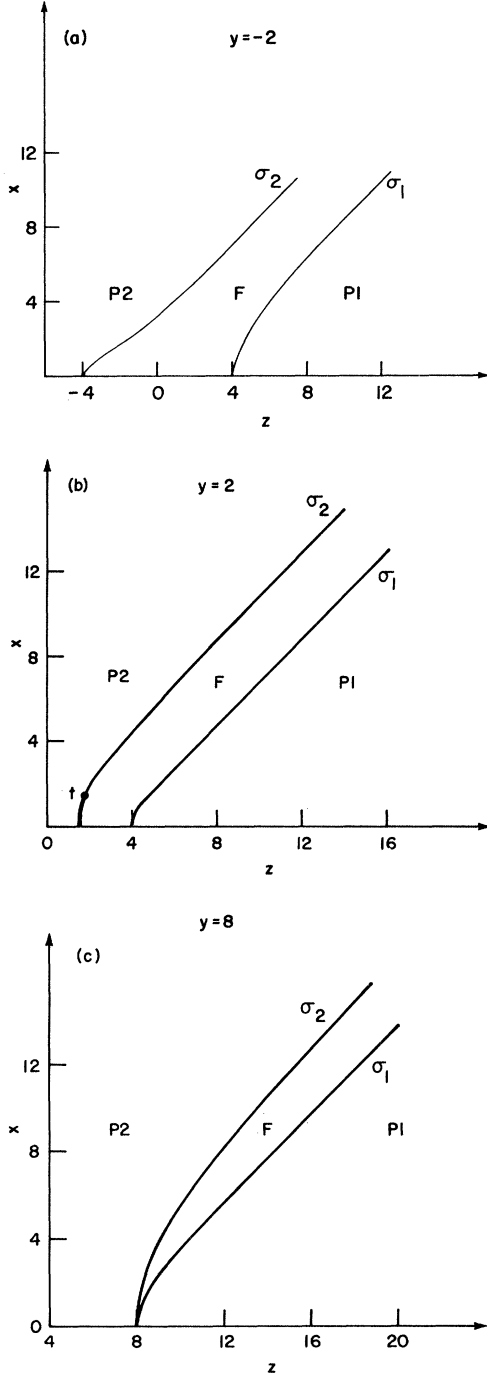


FIG. 3. Sections of the phase diagram of Fig. 2, showing the intersections of σ_1 and σ_2 with the $y = \text{const}$ planes. (a) A typical $y < 0$ section: $y = -2$, exhibiting two second-order lines starting at $x = 0, z = \pm 4$; (b) a typical $0 < y < 4$ section: $y = +2$. Here, the line associated with σ_2 starts at $4(\sqrt{2} - 1) \approx 1.65$ and has a small first-order portion (thick) separated by a tricritical point t from the second-order part; (c) a typical $y > 4$ section: $y = +8$. Here σ_1 and σ_2 start from the same point, $z = 8$, and are second-order throughout.

different RG recursion relations are generated in different regions of the parameter space and it is not clear how to generate continuous global RG flows.

We now apply the results of the quantum model to the weakly interacting classical chain system. We first simplify the general relations (3)–(5) to the relevant case $J_\perp \ll J_\parallel$. We shall also assume $0 < K_\parallel \ll J_\parallel$. To leading order in $e^{-\beta(J_\parallel + K_\parallel)}$, Eqs. (3)–(5) take the form

$$x^2 = \frac{2}{(\beta J_\perp)^2} e^{-\beta(J_\parallel + K_\parallel)}, \quad (26)$$

$$z = \frac{\beta J_\perp}{2} x^2, \quad (27)$$

$$y = (\Delta - J_\parallel - K_\parallel)/J_\perp, \quad (28)$$

where the normalized variables [see Eq. (7c)] were used. As $T \rightarrow 0$, the classical model (1), with $K_\perp = 0$, maps onto the $x = z = 0$ line of the quantum model where y is determined by Eq. (28). With increasing T , the parameters x and z become nonzero [see Eqs. (26) and (27)] while y stays constant. Thus as the temperature is varied a given classical model will map into a steep parabolic line (26)–(28) in the $y = \text{const}$ plane. The intersection of the surface spanned by these lines with the phase transition surfaces, σ_1 and σ_2 , define the phase transition line in the classical model. In fact, since the original transformation to Eq. (7b) holds only for $\beta J_\perp \ll 1$, $z \ll x^2$, the classical surface will intersect *only* with the σ_2 surface. At this intersection, $x \leq O(1)$, see Figs. 2 and 3.

Note, that the condition $\Delta - J_\parallel - K_\parallel \sim J_\perp$ [or equivalently $y = O(1)$] is also required for the transformation to the quantum model to hold. To a leading approximation one can find T_c by neglecting z , obtaining the value of x for which the transition occurs for the given value of y and solving Eq. (26) for β . It is interesting to note that in the limit $J_\perp/J_\parallel \rightarrow 0$, the transition temperature satisfies $T_c \rightarrow 0$, unlike the usual mean-field approximation.^{12–15,35} In Fig. 4 we plot $T_c/[J_\parallel + (d-1)J_\perp]$ as a function of $\Delta/[J_\parallel + (d-1)J_\perp]$ for $d = 2$, and for several values of J_\perp/J_\parallel . Also shown is the analogous curve corresponding to the ordinary mean-field approximation of the BEG model.¹⁴ The latter curve is of course independent of the ratio J_\perp/J_\parallel . Each transition line has a second-order (thin line) and a first-order (thick line) segment joined at a tricritical point. As J_\perp/J_\parallel decreases, the transition temperature is lowered and, *in addition, the first-order segment shrinks*. In fact, the first-order transition occurs only for

$$\left| \frac{\Delta}{J_\parallel + J_\perp} - 1 \right| \leq O\left(\frac{J_\perp}{J_\parallel}\right). \quad (29)$$

This is a rather interesting result since it implies that for weakly coupled chain systems the first-order transition occurs only within a narrow range of the

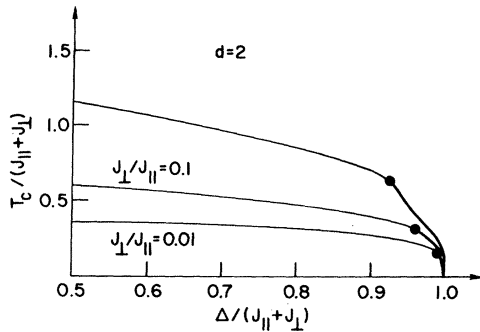


FIG. 4. Phase diagram of the $d=2$ classical model (1) showing $k_B T_c / (J_{\parallel} + J_{\perp})$ as a function of $\Delta / (J_{\parallel} + J_{\perp})$. The upper curve is the result of the ordinary mean-field theory of the BEG model. The lower two curves display the results of our mean-field approximation for $J_{\perp}/J_{\parallel}=0.1, 0.01$. As $J_{\perp}/J_{\parallel} \rightarrow 0$ the tricritical point approaches $(T_c=0, \Delta=J_{\parallel})$.

parameters of the model. Note that $\Delta/J_{\parallel} < 1$ is the condition for the single chain to be ferromagnetic at $T=0$. Equation (29) therefore implies that as long as the single chain is ferromagnetic at $T=0$, the transition is second order for sufficiently small J_{\perp}/J_{\parallel} . This is due to the fact that in the region $\Delta/J_{\parallel} < 1$ and for sufficiently low temperatures the $S=0$ state is

highly unfavored for the single chain, and the model is equivalent to an effective $S = \frac{1}{2}$ Ising system. One would therefore expect such systems to almost always exhibit second-order transitions.

To summarize, we have analyzed the global phase diagram of the $S=1$ Ising model in a transverse field using the mean field-approximation. The applicability of real-space quantum renormalization-group methods for studying the phase diagram is discussed. In applying our results for weakly interacting classical Ising chains, we find that these systems are expected to yield second-order transitions, except for a narrow range of the parameter space, in which the transition is first order.

ACKNOWLEDGMENTS

Part of this work has been carried out at Brookhaven National Laboratory. We thank our colleagues at the Department of Physics for their hospitality. We also thank A. Aharony, N. Berker, E. Domany, V. J. Emery, H. Hamber, and L. Masperi for discussions and correspondence. This work was supported in part by the U.S.-Israel Binational Science Foundation (BSF), Jerusalem, Israel.

*On leave from Tel-Aviv University, Ramat Aviv, Israel.

†On leave from the Weizmann Institute of Science, Rehovot, Israel.

¹L. J. de Jongh and A. R. Miedema, *Adv. Phys.* **23**, 1 (1974).

²M. Steiner, J. Villain, and C. G. Windsor, *Adv. Phys.* **25**, 87 (1976).

³N. Achiwa, *J. Phys. Soc. Jpn.* **27**, 561 (1969).

⁴D. E. Cox and V. J. Minkiewicz, *Phys. Rev. B* **4**, 2209 (1971).

⁵V. J. Minkiewicz, D. E. Cox, and G. Shirane, *Solid State Commun.* **8**, 1001 (1970).

⁶T. Smith and S. A. Friedberg, *Phys. Rev.* **176**, 660 (1968).

⁷F. Borsa and M. Mali, *Phys. Rev. B* **9**, 2215 (1974).

⁸A. V. Shvarts and G. D. Efremova, *Russ. J. Phys. Chem.* **44**, 614 (1970).

⁹B. Widom, *J. Phys. Chem.* **77**, 2196 (1973).

¹⁰R. B. Griffiths, *J. Chem. Phys.* **60**, 195 (1974).

¹¹S. Krinsky and D. Mukamel, *Phys. Rev. B* **11**, 399 (1975); **12**, 211 (1975).

¹²J. Sivardière and J. Lajzerowicz, *Phys. Rev. A* **11**, 2090, 2101 (1975).

¹³D. Furman, S. Dattagupta, and R. B. Griffiths, *Phys. Rev. B* **15**, 441 (1977).

¹⁴M. Blume, V. J. Emery, and R. B. Griffiths, *Phys. Rev. A* **4**, 1071 (1971), and references therein; J. Bernasconi and F. Rys, *Phys. Rev. B* **4**, 3045 (1971).

¹⁵D. Mukamel and M. Blume, *Phys. Rev. A* **10**, 610 (1974).

¹⁶J. L. Cardy and D. J. Scalapino, *Phys. Rev. B* **19**, 1 (1979).

¹⁷E. Simanek, *Solid State Commun.* **31**, 419 (1979); **B**.

Abeles, *Phys. Rev. B* **15**, 2828 (1977). A related $S=1$ model was considered by P. G. deGennes (unpublished).

¹⁸E. K. Riedel and F. J. Wegner, *Phys. Rev. Lett.* **29**, 349 (1972); *Phys. Rev. B* **7**, 248 (1973).

¹⁹D. M. Saul, M. Wortis, and D. Stauffer, *Phys. Rev. B* **9**, 4964 (1974).

²⁰B. L. Arora and D. P. Landau, in *Magnetism and Magnetic Materials—1972*, edited by C. D. Graham and J. J. Rhyne, AIP Conf. Proc. No. 10 (AIP, New York, 1973), p. 870.

²¹S. Krinsky and D. Furman, *Phys. Rev. Lett.* **32**, 731 (1979); *Phys. Rev. B* **11**, 2602 (1975).

²²A. N. Berker and M. Wortis, *Phys. Rev. B* **14**, 4946 (1976), and references therein.

²³M. Kac, *Phys. Fluids* **2**, 8 (1959).

²⁴D. J. Scalapino, M. Sears, and R. A. Ferrell, *Phys. Rev. B* **6**, 3409 (1972).

²⁵M. Suzuki, *Prog. Theor. Phys.* **46**, 1337 (1971); **56**, 1454 (1976).

²⁶Z. Friedman, *Phys. Rev. Lett.* **36**, 1326 (1976).

²⁷K. Subbarao, *Phys. Rev. Lett.* **37**, 1712 (1976).

²⁸B. Stoekley and D. J. Scalapino, *Phys. Rev. B* **11**, 205 (1975).

²⁹S. Jafarey, R. Pearson, D. J. Scalapino, and B. Stoekley (unpublished).

³⁰S. D. Drell, M. Weinstein, and S. Yankielovicz, *Phys. Rev. D* **14**, 487 (1976).

³¹R. Jullien, J. N. Fields, and S. Doniach, *Phys. Rev. Lett.* **38**, 1500 (1977); *Phys. Rev. B* **16**, 4889 (1977).

³²R. Jullien, P. Pfeuty, J. N. Fields, and S. Doniach, *Phys.*

- Rev. B 18, 3568 (1978).
- ³³R. Jullien and P. Pfeuty, Phys. Rev. B 19, 4646 (1979).
- ³⁴K. Penson, R. Jullien, and P. Pfeuty, Phys. Rev. B 19, 4653 (1979).
- ³⁵D. J. Scalapino, Y. Imry, and P. Pincus, Phys. Rev. B 11, 2042 (1975).
- ³⁶H. Hamber, Phys. Rev. B 21, 3999 (1980).
- ³⁷B. Hu, Phys. Lett. 75A, 372 (1980).
- ³⁸D. Boyanovsky and L. Masperi, Phys. Rev. D 21, 1550 (1980).
- ³⁹M. Kac, in *Proceedings of the 1966 Brandeis Summer Institute*, edited by S. Deser and M. Chretien (Benjamin, New York, 1967).